Integrated Catalytic Conversion of γ-Valerolactone to Liquid Alkenes for Transportation Fuels

Jesse Q. Bond, *et al.*

Science **327**, 1110 (2010);
DOI: 10.1126/science.1184362

control of the *TMR* with the ferroelectric polarization is repeatable, as shown in Fig. 4 for junction #1 where *TMR* curves are recorded after poling the ferroelectric up, down, up, and down, sequentially (*28*).

For tunnel junctions with a ferroelectric barrier and dissimilar ferromagnetic electrodes, we have reported the influence of the electrically controlled ferroelectric barrier polarization on the tunnel-current spin polarization. This electrical influence over magnetic degrees of freedom represents a new and interfacial magnetoelectric effect that is large because spin-dependent tunneling is very sensitive to interfacial details. Ferroelectrics can provide a local, reversible, nonvolatile, and potentially low-power means of electrically addressing spintronics devices.

References and Notes

1. C. Chappert, A. Fert, F. N. Van Dau, *Nat. Mater.* **6**, 813 (2007).
2. I. Žutić, J. Fabian, S. Das Sarma, *Rev. Mod. Phys.* **76**, 323 (2004).
3. J. C. Slonczewski, *J. Magn. Magn. Mater.* **159**, L1 (1996).
4. J. Nitta, T. Akazaki, H. Takayanagi, T. Enoki, *Phys. Rev. Lett.* **78**, 1335 (1997).
5. H. Ohno *et al.*, *Nature* **408**, 944 (2000).
6. D. Chiba *et al.*, *Nature* **455**, 515 (2008).
7. M. Weisheit *et al.*, *Science* **315**, 349 (2007).
8. T. Maruyama *et al.*, *Nat. Nanotechnol.* **4**, 158 (2008).
9. S. W. E. Riester *et al.*, *Appl. Phys. Lett.* **94**, 063504 (2009).
10. I. Stolichnov *et al.*, *Nat. Mater.* **7**, 464 (2008).
11. C. Bihler *et al.*, *Phys. Rev. B* **78**, 045203 (2008).
12. M. Overby, A. Chernyshov, L. P. Rokhinson, X. Liu, J. K. Furdyna, *Appl. Phys. Lett.* **92**, 192501 (2008).
13. C. Thiele, K. Dörr, O. Bilani, J. Rödel, L. Schultz, *Phys. Rev. B* **75**, 054408 (2007).
14. W. Eerenstein, M. Wiora, J. L. Prieto, J. F. Scott, N. D. Mathur, *Nat. Mater.* **6**, 348 (2007).
15. T. Kanki, H. Tanaka, T. Kawai, *Appl. Phys. Lett.* **89**, 242506 (2006).
16. Y.-H. Chu *et al.*, *Nat. Mater.* **7**, 478 (2008).
17. S. Sahoo *et al.*, *Phys. Rev. B* **76**, 092108 (2007).
18. C.-G. Duan, S. S. Jaswal, E. Y. Tsymbal, *Phys. Rev. Lett.* **97**, 047201 (2006).
19. M. Fechner *et al.*, *Phys. Rev. B* **78**, 212406 (2008).
20. J. Lee, N. Sai, T. Cai, Q. Niu, A. A. Demkov, preprint available at http://arxiv.org/abs/0912.3492v1.
21. K. Yamauchi, B. Sanyal, S. Picozzi, *Appl. Phys. Lett.* **91**, 062506 (2007).
22. M. K. Niranjan, J. P. Velev, C.-G. Duan, S. S. Jaswal, E. Y. Tsymbal, *Phys. Rev. B* **78**, 104405 (2008).
23. M. Jullière, *Phys. Lett. A* **54**, 225 (1975).
24. J. F. Scott, *Science* **315**, 954 (2007).
25. M. Bowen *et al.*, *Appl. Phys. Lett.* **82**, 233 (2003).
26. J. P. Velev *et al.*, *Nano Lett.* **9**, 427 (2009).
27. F. Yang *et al.*, *J. Appl. Phys.* **102**, 044504 (2007).
28. Materials and methods are available as supporting material on *Science* Online.
29. V. Garcia *et al.*, *Nature* **460**, 81 (2009).
30. K. J. Choi *et al.*, *Science* **306**, 1005 (2004).
31. K. Bouzehouane *et al.*, *Nano Lett.* **3**, 1599 (2003).
32. T. J. Regan *et al.*, *Phys. Rev. B* **64**, 214422 (2001).
33. N. Hollmann *et al.*, *Phys. Rev. B* **80**, 085111 (2009).
34. M. Abbate *et al.*, *Phys. Rev. B* **44**, 5419 (1991).
35. E. Y. Tsymbal, H. Kohlstedt, *Science* **313**, 181 (2006).
36. M. Ye. Zhuravlev, R. F. Sabirianov, S. S. Jaswal, E. Y. Tsymbal, *Phys. Rev. Lett.* **94**, 246802 (2005).
37. M. Ye. Zhuravlev, R. F. Sabirianov, S. S. Jaswal, E. Y. Tsymbal, *Phys. Rev. Lett.* **102**, 169901 (2009).
38. H. Kohlstedt, N. A. Pertsev, J. Rodriguez Contreras, R. Waser, *Phys. Rev. B* **72**, 125341 (2005).
39. M. Gajek *et al.*, *Nat. Mater.* **6**, 296 (2007).
40. M. Bowen *et al.*, *Phys. Rev. Lett.* **95**, 137203 (2005).
41. J. D. Burton, E. Y. Tsymbal, *Phys. Rev. B* **80**, 174406 (2009).

42. We thank R. Guillemet, C. Israel, M. E. Vickers, R. Mattana, J.-M. George, and P. Seneor for technical assistance, and C. Colliex for fruitful discussions on the microscopy measurements. This study was partially supported by the France-U.K. Partenariat Hubert Curien Alliance program, the French Réseau Thématique de Recherche Avancée Triangle de la Physique, the European Union (EU) Specific Targeted Research Project (STReP) Manipulating the Coupling in Multiferroic Films, EU STReP Controlling Mesoscopic Phase Separation, U.K. Engineering and Physical Sciences Research Council grant EP/E026206/I, French C-Nano Île de France, French Agence Nationale de la Recherche (ANR) Oxitronics, French ANR Alicante, the European Enabling Science and Technology through European Elelctron Microscopy program, and the French Microscopie Electronique et Sonde Atomique network. X.M. acknowledges support from Comissionat per a Universitats i Recerca (Generalitat de Catalunya).

Supporting Online Material

www.sciencemag.org/cgi/content/full/science.1184028/DC1
Materials and Methods
Figs. S1 to S5
References

30 October 2009; accepted 4 January 2010
Published online 14 January 2010;
10.1126/science.1184028
Include this information when citing this paper.

Integrated Catalytic Conversion of γ-Valerolactone to Liquid Alkenes for Transportation Fuels

Jesse Q. Bond, David Martin Alonso, Dong Wang, Ryan M. West, James A. Dumesic*

Efficient synthesis of renewable fuels remains a challenging and important line of research. We report a strategy by which aqueous solutions of γ-valerolactone (GVL), produced from biomass-derived carbohydrates, can be converted to liquid alkenes in the molecular weight range appropriate for transportation fuels by an integrated catalytic system that does not require an external source of hydrogen. The GVL feed undergoes decarboxylation at elevated pressures (e.g., 36 bar) over a silica/alumina catalyst to produce a gas stream composed of equimolar amounts of butene and carbon dioxide. This stream is fed directly to an oligomerization reactor containing an acid catalyst (e.g., H ZSM-5, Amberlyst-70), which couples butene monomers to form condensable alkenes with molecular weights that can be targeted for gasoline and/or jet fuel applications. The effluent gaseous stream of CO_2 at elevated pressure can potentially be captured and then treated or sequestered to mitigate greenhouse gas emissions from the process.

Diminishing fossil fuel resources and increasing amounts of CO_2 in the atmosphere require the development and implementation of strategies for the production of renewable transportation fuels (*1*–*4*). Although first-generation biofuels, such as corn ethanol and biodiesel, have the capacity to mitigate worldwide dependence on petroleum, new processes using lignocellulosic biomass must be developed to produce sustainable biofuels to meet worldwide demand (*5*). In this respect, γ-valerolactone (GVL) has been identified as a renewable platform molecule (*6*) with potential impact as a feedstock in the production of both energy (*6*, *7*) and fine chemicals (*8*). GVL is produced by hydrogenation of levulinic acid, which can be produced, potentially at low cost, from agricultural waste (*3*) by processes already demonstrated on a commercial scale (*9*). Recently, researchers have minimized the demand for an external source of hydrogen in this process by using the formic acid formed in equimolar amounts with levulinic acid through decomposition of cellulose (*7*) and C_6 sugars (*10*).

GVL retains 97% of the energy content of glucose and performs comparably to ethanol when used as a blending agent (10% v/v) in conventional gasoline (*6*). It has also been applied as a renewable cosolvent in splash blendable diesel fuel (*11*). GVL suffers, however, from several limitations for widespread use in the transportation sector, such as high water solubility, blending limits for use in conventional combustion engines, and lower energy density compared to petroleum-derived fuels. Although these limitations can be at least partially alleviated by reduction of GVL with an external source of hydrogen to produce methyltetrahydrofuran (*12*), which can be blended up to 70% in gasoline (*3*), the limitations would be completely eliminated by converting GVL to liquid alkenes (or alkanes) with molecular weights targeted for direct use as gasoline, jet, and/or diesel fuels.

Regarding the economic feasibility and environmental impact of biofuels, two commonly cited considerations are the demand for external hydrogen in producing a surrogate fuel and CO_2 emissions arising from its combustion (*13*). By processing GVL with a combined decarboxylation and oligomerization strategy, it is possible to

Department of Chemical and Biological Engineering, University of Wisconsin-Madison, Madison, WI 53706, USA.

*To whom correspondence should be addressed. E-mail: dumesic@engr.wisc.edu

mitigate both concerns simultaneously. As shown in the stoichiometric relations below (Eq. 1), the conversion of GVL to alkenes and CO_2 does not require an external source of hydrogen:

$$C_5O_2H_8 \longrightarrow C_4H_8 + CO_2$$
$$C_4H_8 \longrightarrow \sum_{n=2}^{5} \frac{1}{n}[C_nH_{8n}] \qquad (1)$$

(The hydrogenation of an alkene to an alkane requires one equivalent of H_2; however, the amount of H_2 required for the overall conversion of GVL to an alkane decreases as the molecular weight of the alkane increases.) Although the combustion of biomass-derived alkenes is equivalent to the combustion of GVL in terms of energy, an additional advantage in isolating the alkenes is that the first equivalent of CO_2 in Eq. 1 can be liberated under conditions more conducive to capture than in an automotive or jet engine. The same argument can be used to describe the conversion of glucose to ethanol, as indicated in the stoichiometric relation below (Eq. 2):

$$C_6O_6H_{12} \longrightarrow 2C_2OH_6 + 2CO_2 \qquad (2)$$

However, an important difference between these two approaches for the production of biofuels is that the conversion of GVL to alkenes can produce a CO_2 stream at elevated pressure (e.g., 36 bar, as demonstrated in this report), appropriate for sequestration (*14*, *15*), conversion to methanol (*16*, *17*) upon reaction with a renewable source of hydrogen (*18*, *19*), or copolymerization with epoxides to yield polycarbonates (*20*, *21*). By contrast, the production of CO_2 during fermentation of glucose to ethanol is carried out at atmospheric pressure in the presence of air (*22*).

Figure 1 shows our integrated approach to convert GVL in aqueous solution to liquid alkenes with molecular weights appropriate for transportation fuels. The sequence entails catalytic decarboxylation of GVL to butene and CO_2, combined with the oligomerization of butene at elevated pressures, with a single catalytic system involving two tubular flow reactors connected in series with an interreactor separator (*23*). The first step is the ring opening of GVL to produce an isomeric mixture of unsaturated pentenoic acids, which can then undergo decarboxylation to produce butene isomers and a stoichiometric quantity of CO_2. We demonstrate here that both of these transformations can be carried out over a solid acid catalyst, SiO_2/Al_2O_3, in the presence of water in a single, fixed bed reactor. Moreover, these reactions can be carried out at pressures ranging from ambient to 36 bar. After a separation step in which water is condensed to the liquid state, the butene/CO_2 gas stream is upgraded in a second reactor to higher molecular weight alkenes through acid-catalyzed oligomerization (*24*, *25*). This oligomerization process is favored at elevated pressures and can be tuned to yield alkenes with a targeted range of molecular weights and varied degrees of branching in the product stream (*26*, *27*). In a second separation step, the alkenes are condensed to form a liquid product stream, while CO_2 remains as a high-pressure gas. This approach does not require an external source of hydrogen as is necessary, for example, in the catalytic upgrading of bio-oils produced by pyrolysis of biomass (*28*).

Table 1 summarizes effects of pressure, temperature, and feed composition for the conversion of aqueous solutions of GVL to butene and CO_2 over a SiO_2/Al_2O_3 catalyst (*23*). For a given temperature (entries 1 to 3), the conversion of GVL is approximately constant at pressures ranging from 1 to 36 bar; however, the yield of butenes decreases at higher pressures. Increased pressure has minimal effect on the ring opening (conversion) of GVL; however, the rate of decarboxylation of the reactive intermediate, pentenoic acid (Fig. 1), is hindered at elevated pressures. As system pressure increases, we observe a loss of selectivity to butene and a corresponding increase in selectivity to pentenoic acid. We propose that GVL decarboxylation proceeds through acid-catalyzed protonation to cleave the cyclic ester linkage, followed by proton transfer leading to C-C bond scission and deprotonation to yield butene and an equivalent of CO_2 [see fig. S4 and related text (*23*)]. The selectivity to butene can be improved by operating the reactor at higher temperatures, and good yields of butene (60%) were observed at 673 K and 36 bar (entry 4); however, higher temperature leads to coke formation, likely by polymerization of pentenoic acid, which causes catalyst deactivation with time on stream. Increasing the concentration of GVL in the feed has a positive effect on butene yield (entries 5 and 6), although coke formation eventually becomes problematic, leading to catalyst deactivation at GVL concentrations higher than 80 weight % (wt %) [figs. S1 and S2 and related text (*23*)]. Deactivation of SiO_2/Al_2O_3 is reversible, and catalytic activity can be restored by calcination at 723 K. An appropriate compromise between obtaining a high rate of GVL conversion and maintaining stable catalyst operation is achieved with an aqueous feed solution containing 60 wt % GVL at 648 K and at a pressure of 36 bar (entry 5). Under these conditions, catalytic activity remains constant for more than 100 hours of time on stream [fig. S2 (*23*)]. We observe 85% conversion of the GVL feed to form butene and stoichiometric CO_2 (67% yield), pentenoic acid isomers (15% yield), small oxygenates such as butanol and propionaldehyde (2% yield), and aromatization or oligomerization products including octene and ethylbenzene (1% yield). The butene yield is limited by the unconverted pentenoic acid intermediate, and yields >90% are achieved with a 60 wt % feed at lower space velocities (entry 7) with 100% of GVL conversion. Under these conditions, pentenoic acid is not observed, and 93% yield to butene is achieved. The fraction of butene converted to C_{8+} alkenes and aromatics increases and accounts for the remainder of products observed (7% yield). The percentage of butene present as 1-butene (33%) compared to and cis/trans 2-butene (67%) is higher than at thermodynamic equilibrium, suggesting that 1-butene is the primary product.

The effluent from the GVL decarboxylation reactor is a mixture of butene, CO_2, and water at elevated temperature and pressure. This mixture must subsequently be passed to the butene oligomerization reactor, operating at lower temperature to favor alkene coupling and minimize cracking

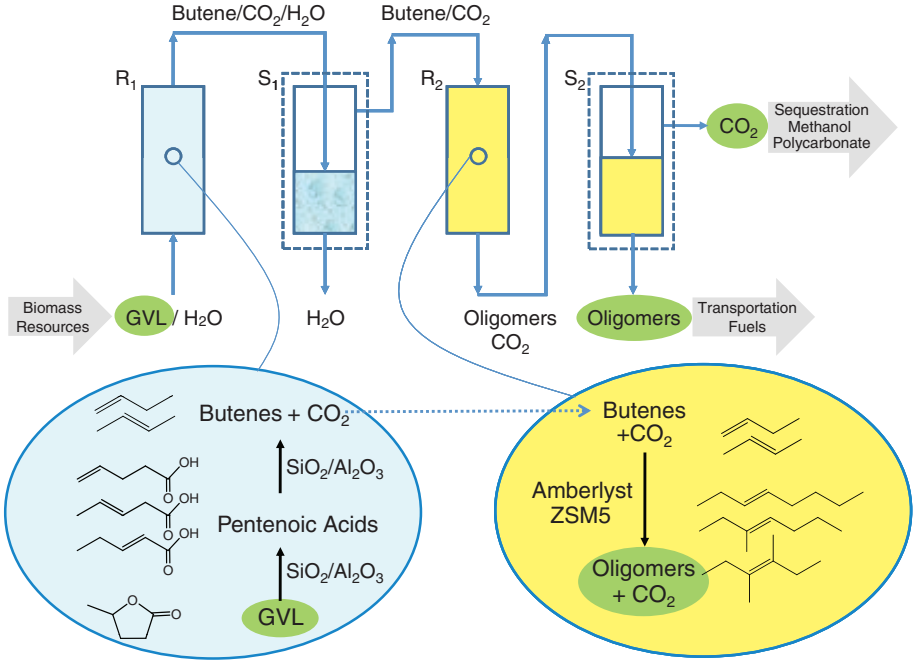

Fig. 1. Reaction pathways for conversion of GVL to butenes and CO_2, and the integrated conversion of GVL to both a liquid stream of alkenes for use in transportation fuels and a gaseous stream rich in CO_2 that is appropriate for further processing options.

reactions. Although the oligomerization of alkenes is practiced widely in the petrochemical industry (*24*, *25*, *29*), we found no reports of processing butene/CO_2 mixtures in the presence of water at elevated pressures, thus necessitating studies to identify catalysts and reaction conditions for our integrated catalytic process. Table 2 summarizes experimental results for butene oligomerization with HZSM-5 and Amberlyst-70 as catalysts (*23*). The conversion of butene over HZSM-5 reaches ~50% at ambient pressure and moderate temperature (523 K, entry 1). Higher conversions are achieved by increasing the reaction temperature to 573 K (entry 2); however, a larger fraction of the products observed are low molecular weight alkenes, produced via cracking, and the selectivity for desired products (C_{8+} alkenes for jet fuel applications) decreases from 80 to 55%. Increasing the pressure to 17 bar leads to an increase in the conversion of butene, accompanied by a decrease in selectivity for C_{8+} alkenes (entry 3). Higher selectivities (>88%) can be achieved at elevated pressure (17 bar) by decreasing the temperature to 498 K (entry 4). A further decrease in temperature to 473 K leads to minimal improvement in selectivity but causes a decrease in butene conversion (entry 5). An increase in pressure to 36 bar at 498 K allows for high overall yields of C_{8+} alkenes (77%) at high butene conversion (87%) (entry 6).

The addition of an equimolar co-feed of CO_2 to the butene oligomerization reactor leads to a decrease in butene conversion (entry 7), although the selectivity to C_{8+} alkenes remains unchanged. This decrease in butene conversion is caused by the corresponding decrease in butene partial pressure in the reactor, and the initial activity is restored upon removal of CO_2 from the feed (entry 8). The conversion of butene can be increased to 90% in the presence of an equimolar amount of CO_2, without modifying the selectivity to C_{8+} alkenes, by decreasing the weight hourly space velocity (WHSV) to 0.09 $hour^{-1}$ (entry 9). Low amounts of water in the feed decrease the conversion of butene from 90 to 82% (entry 10). As the concentration of water in the oligomerization feed increases, inhibition becomes more pronounced, and only 47% of the butene is converted when equimolar quantities of butene, CO_2, and water are fed to the reactor. When the water co-feed is stopped after 100 hours time on stream [supporting online material (SOM) Text (*23*)], 96% of the initial activity is recovered, indicating reversible inhibition and long-term stability. In all experiments reported using HZSM-5 at 498 K, the selectivity to C_{8+} alkenes is higher than 85%, indicating minimal extent of cracking.

Complete butene conversion can be achieved over Amberlyst-70 with high selectivity to C_{8+} oligomers at elevated space velocities (0.63 $hour^{-1}$, entry 14). The conversion of butene decreases upon introducing an equimolar co-feed of CO_2 (entry 15), as found for HZSM-5. The inhibiting effect of water is minimal at low feed concentrations (entry 16). As the fraction of water in the feed increases, inhibition becomes more pronounced, and complete loss of activity is observed at high amounts of water (entries 17 and 18). When the co-feed of water is stopped after 100 hours time on stream [SOM Text (*23*)], Amberlyst-70 regains 100% of its initial activity.

Results from Tables 1 and 2 suggest that GVL decarboxylation can be coupled with butene oligomerization in a single system at elevated pressures, thereby reducing the overall capital expenditure that would be required to separate, purify, and pressurize the butene obtained from GVL. Another advantage of the integrated system is that the vapor pressure of the CO_2 co-product formed by GVL decarboxylation is sufficiently high to achieve and sustain elevated system pressures appropriate for oligomerization,

Table 1. GVL conversion and butene yield at different reaction conditions over a SiO_2/Al_2O_3 catalyst operating at a weight hourly space velocity (WHSV) equal to 0.9 $hour^{-1}$.

Entry	*T* (K)	*P* (bar)	Feed GVL concentration (wt %)	GVL conversion (%)	Butene yield (%)
1	648	1	30	97	75
2	648	18	30	94	65
3	648	36	30	70	35
4	673	36	30	95	60
5	648	36	60	85	67
6	648	36	80	99	96
7*	648	36	60	99	93

*WHSV = 0.18 $hour^{-1}$

Table 2. 1-Butene conversion, selectivity, and yield to liquid C_8-C_{16} alkenes (hydrocarbons of appropriate molecular weight for direct use in liquid transportation fuels) and C_{8+} alkenes (distribution includes all the above class in addition to all oligomers larger than C_{16}) over HZSM-5 and Amberlyst-70 catalysts.

Entry	Catalyst	Feed composition	*T* (K)	*P* (bar)	Butene conversion (%)	Liquid selectivity ($C_8 - C_{16}$)/C_{8+} alkenes (%)	Liquid yield ($C_8 - C_{16}$)/C_{8+} alkenes (%)
1*	HZSM-5	Butene	523	1	51	77/80	40/41
2*	HZSM-5	Butene	573	1	87	50/55	43/48
3*	HZSM-5	Butene	523	17	90	59/73	53/66
4*	HZSM-5	Butene	498	17	64	78/88	50/56
5*	HZSM-5	Butene	473	17	38	89/91	34/35
6*	HZSM-5	Butene	498	36	87	82/88	71/77
7*	HZSM-5	Butene/CO_2 50/50	498	36	64	77/85	49/54
8*	HZSM-5	Butene	498	36	90	80/89	72/80
9†	HZSM-5	Butene/CO_2 50/50	498	17	90	65/88	58/79
10†	HZSM-5	Butene/CO_2/H_2O 47.5/47.5/5	498	17	82	72/89	59/73
11†	HZSM-5	Butene/CO_2/H_2O 45/45/10	498	17	72	72/86	52/62
12†	HZSM-5	Butene/CO_2/H_2O 33/33/33	498	17	47	79/89	37/42
13†	HZSM-5	Butene/CO_2 50/50	498	17	86	78/93	67/80
14‡	Amberlyst 70	Butene	443	17	99	72/96	71/95
15‡	Amberlyst 70	Butene/CO_2 50/50	443	17	93	69/95	64/88
16‡	Amberlyst 70	Butene/CO_2/H_2O 47.5/47.5/5	443	17	90	74/95	66/86
17‡	Amberlyst 70	Butene/CO_2/H_2O 45/45/10	443	17	50	85/92	43/46
18‡	Amberlyst 70	Butene/CO_2/H_2O 33/33/33	443	17	0	—	—
19‡	Amberlyst 70	Butene/CO_2 50/50	443	17	93	58/93	54/87

*WHSV = 0.11 $hour^{-1}$. †WHSV =0.09 $hour^{-1}$. ‡WHSV = 0.63 $hour^{-1}$.

Table 3. Performance of integrated catalytic system consisting of two flow reactors in series with an interreactor separator. Second reactor operated at 36 bar.

Entry	Reactor 1 (GVL to butene)				Reactor 2 (butene to alkenes)				GVL to liquid (C_8-C_{16})/ C_{8+}(%)
	T (K)	GVL conversion (%)	Butene yield (%)	Butene out of first separator (%)	Catalyst	*T* (K)	Butene conversion (%)	Liquid selectivity to (C_8-C_{16})/ C_{8+} (%)	
1*	648	63	37	75	HZSM-5 (14 g)	498	95	63/90	17/24
2†	648	98	91	90	HZSM-5 (14 g)	498	44	76/86	28/31
3†	648	99	92	88	Amberlyst (3 g)	443	92	74/94	50/62
4‡	648	99	90	89	Amberlyst (4 g)	443	94	64/93	48/66
5§	648	99	94	93	Amberlyst (4 g)	443	81	79/94	53/63
6‖	648	99	98	95	Amberlyst (12 g)	443	90	75/95	60/77

*Reactor 1: 2.7 g SiO_2-Al_2O_3.WHSV = 0.68 hour^{-1}. First separator at 373 K. †Reactor 1: 10 g SiO_2-Al_2O_3.WHSV = 0.18 hour^{-1}. First separator at 383 K. ‡Reactor 1: 10 g SiO_2-Al_2O_3. WHSV = 0.18 hour^{-1}. First separator at 388 K. §Reactor 1: 10 g SiO_2-Al_2O_3.WHSV = 0.22 hour^{-1}. First separator at 398 K. ‖Reactor 1: 8 g SiO_2-Al_2O_3.WHSV = 0.22 hour^{-1}. First separator at 398 K.

which eliminates the need for external compression strategies in continuous operation. Because water has a strong negative effect on oligomerization, the reaction system depicted in Fig. 1 was designed to carry out the desired conversion of GVL to liquid alkenes by including a separation unit between the GVL decarboxylation reactor and the butene oligomerization reactor to minimize the amount of water carried downstream. This system allows a high-pressure stream of gaseous butene to be delivered from the first separator to the inlet of the oligomerization reactor, while >98% of the water in the effluent from the first reactor is removed as a liquid. The total pressure of the system is set at 36 bar, a value that is appropriate for GVL conversion (Table 1) as well as for butene oligomerization (Table 2), and the temperature of the interreactor separator is set at a value (e.g., 373 to 398 K) that is sufficiently low to liquefy most of the water for removal but sufficiently high to maintain butene in the gaseous state for transfer to the oligomerization reactor. The products from the second reactor are collected in a second phase separator operating at ambient temperature, producing a liquid effluent stream of C_{8+} alkenes and unreacted butene, and a gaseous effluent stream of CO_2 with trace quantities of organic compounds.

Table 3 shows results for the conversions of GVL and butene in the integrated catalytic system depicted in Fig. 1 (*23*). [The product distributions for the liquid alkene effluent streams of these experiments are presented in table S2 (*23*).] The conversion of GVL and yield of butene in the first reactor, as well as butene conversion and selectivity to liquid C_{8+} alkenes in the second reactor, are similar in the integrated system (entry 1) to those values obtained for the isolated processes operating at similar conditions (Tables 1 and 2), illustrating the reproducibility of the experiments. This experiment was carried out for 85 hours [fig. S3 (*23*)] while the interreactor separator was operated at 373 K and a pressure of 36 bar; under these conditions, no aqueous phase was observed in the effluent from the oligomerization reactor, and the overall yield from GVL to C_{8+} alkenes was 24%. This overall yield was limited by the decarboxylation of GVL and loss of butene in the first separation step.

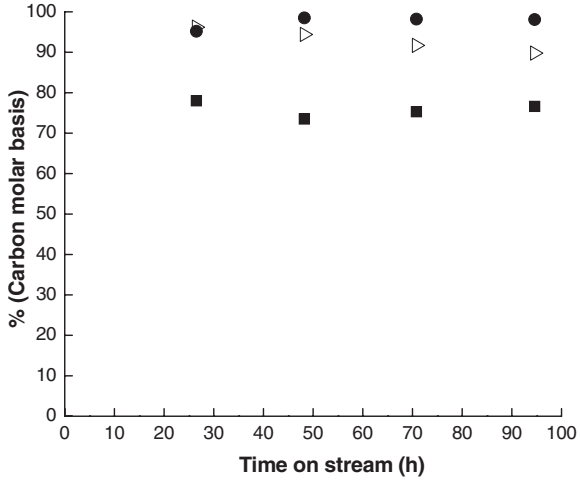

Fig. 2. Yield of butene from GVL in reactor 1 (●), butene conversion in reactor 2 (▷), and overall yield of liquid C_{8+} alkenes from GVL in the integrated process (■) versus time on stream. First reactor operated at 36 bar, 648 K and WHSV = 0.22 hour^{-1}. First separator operated at 36 bar and 398 K. Second reactor operated at 36 bar and 443 K with 12 g of Amberlyst-70. Second separator operated at 36 bar and 298 K.

To increase the total yield to liquid alkenes from GVL, we carried out experiments at lower space velocity of GVL (entry 2) and higher separator temperature (383 K). Under these conditions, GVL is almost quantitatively converted to butene with minimal formation of side products such as C_{8+} alkenes and aromatics. Operating the separator at higher temperature increases the extent of both butene and water vaporization and subsequent delivery to the oligomerization reactor. The increased WHSV of butene in the second reactor, combined with the inhibiting effect of water, causes a decrease in butene oligomerization, although the total yield of C_{8+} oligomers is improved to 31%.

Amberlyst-70 was identified to be a more active oligomerization catalyst than HZSM-5, and it can be used at lower temperatures to decrease the extent of cracking reactions and to improve the oligomerization selectivity to C_{8+} alkenes (Table 2). When Amberlyst-70 is used in the second reactor, the conversion of butene increases to 92%, with 94% selectivity to C_{8+} alkenes. Under these conditions, the total yield of C_{8+} alkenes from GVL increases to 62% (entry 3). The total yield to C_{8+} alkenes can be increased by decreasing the WHSV in the second reactor to increase the butene conversion (entry 4). To maximize the amount of butene delivered to the second reactor, we increased the WHSV in the first reactor from 0.18 to 0.22 hour^{-1}, which decreases decarboxylation by-products, such as higher alkenes and aromatics, and increases the butene yield to 94%. Additionally, by operating the initial separator at 398 K, 93% of the butene formed is delivered to the oligomerization reactor (entry 5). The higher separator temperature increases the amount of water in the second reactor, which inhibits butene oligomerization (81% conversion) and results in an overall yield of C_{8+} alkenes equal to 63%. A final yield over 75% can be achieved by increasing the amount of catalyst in the second reactor to compensate for water inhibition and reducing the amount of catalyst in the first reactor to maintain the same WHSV (entry 6). Under these conditions, the integrated catalytic system operates for more than 90 hours of time on stream (Fig. 2) with high conversions of GVL and butene in the first and second reactors, respectively, and with a high overall yield to C_{8+} alkenes (>75%). Increasing

the amount of catalyst in the oligomerization reactor modifies the selectivity, decreasing the C_8-C_{16} fraction and increasing the percentage of larger alkenes [see table S2 and related text (*23*)].

The integrated system reported here for conversion of GVL to liquid alkenes in the transportation fuel range consists of two flow reactors, two phase separators, and a simple pumping system for delivery of an aqueous solution of GVL, thereby minimizing secondary processing steps and equipment (e.g., purification of feeds, compression and pumping of gases). In addition, this approach does not require the use of precious metal catalysts, further decreasing capital costs. The catalytic system described in this report provides an efficient and inexpensive processing strategy for GVL. The cost of producing either butene or jet fuel with the approaches described here would be governed by the market value of GVL, and further research should be carried out toward optimizing production of GVL from renewable biomass resources, thereby minimizing the cost of the GVL feed to our process, and toward utilization of the high-pressure CO_2 coproduct stream formed in our process. Additionally, the yield of high molecular weight alkenes from GVL would benefit from the development of water-tolerant oligomerization catalysts.

References and Notes

1. E. L. Kunkes *et al.*, *Science* **322**, 417 (2008).
2. A. J. Ragauskas *et al.*, *Science* **311**, 484 (2006).
3. G. W. Huber, S. Iborra, A. Corma, *Chem. Rev.* **106**, 4044 (2006).
4. D. A. Simonetti, J. Rass-Hansen, E. L. Kunkes, R. R. Soares, J. A. Dumesic, *Green Chem.* **9**, 1073 (2007).
5. G. W. Huber, B. E. Dale, *Sci. Am.* **301**, 52 (2009).
6. I. T.Horváth, H. Mehdi, V. Fábos, L. Boda, L. T. Mika, *Green Chem.* **10**, 238 (2008).
7. H. Mehdi *et al.*, *Top. Catal.* **48**, 49 (2008).
8. L. E. Manzer, *Appl. Catal. Gen.* **272**, 249 (2004).
9. S. W. Fitzpatrick, "Final Technical Report: Commercialization of the Biofine Technology for Levulinic Acid Production from Paper Sludge," *Tech. Report No. DOE/CE/41178* (BioMetics, Inc, Waltham, MA, 2002); www.osti.gov/bridge.
10. H. Heeres *et al.*, *Green Chem.* **11**, 1247 (2009).
11. I. Ahmed, U.S. Patent 6,190,427 (2001).
12. D. C. Elliott, J. G. Frye, U.S. Patent 5,883,266 (1999)
13. G. W. Huber, "Breaking the Chemical and Engineering Barriers to Lignocellulosic Biofuels: Next Generation Hydrocarbon Biorefineries" (Univ. of Massachusetts Amherst, 2007); www.ecs.umass.edu/biofuels/Images/Roadmap2-08.pdf.
14. R. S. Haszeldine, *Science* **325**, 1647 (2009).
15. K. S. Lackner, *Science* **300**, 1677 (2003).
16. H. Sakurai, M. Haruta, *Catal. Today* **29**, 361 (1996).
17. J. Toyir, P. R. de la Piscina, J. L. G. Fierro, N. Homs, *Appl. Catal. Environ.* **34**, 255 (2001).
18. S. Koppatz *et al.*, *Fuel Process. Technol.* **90**, 914 (2009).
19. R. D. Cortright, R. R. Davda, J. A. Dumesic, *Nature* **418**, 964 (2002).
20. G. W. Coates, D. R. Moore, *Angew. Chem. Int. Ed.* **43**, 6618 (2004).
21. D. J. Darensbourg, *Chem. Rev.* **107**, 2388 (2007).
22. M. Wick, J. M. Lebeault, *Appl. Microbiol. Biotechnol.* **56**, 687 (2001).
23. Materials and methods are available as supporting material on *Science* Online.
24. S. Matar, L. F. Hatch, *Chemistry of Petrochemical Processes* (Gulf Professional Publishing, Houston, TX, ed. 2, 2000), pp. 248–250.
25. J. Čejka, H. van Bekkum, A. Corma, F. Schüth, in *Introduction to Zeolite Science and Practice* (Elsevier, Amsterdam, rev. ed. 3, 2007), pp. 895–899.
26. A. Mantilla *et al.*, *Catal. Today* **107-108**, 707 (2005).
27. R. J. Quann, L. A. Green, S. A. Tabak, F. J. Krambeck, *Ind. Eng. Chem. Res.* **27**, 565 (1988).
28. G. Centi, R. Van Santen, in *Catalysis for Renewables: From Feedstock to Energy Production* (Wiley-VCH, Weinheim, Germany, 2007), p. 137.
29. J. Skupinska, *Chem. Rev.* **91**, 613 (1991).

30. This work was supported through funding from the Defense Advanced Research Projects Agency (DARPA) (Surf-cat: Catalysts for Production of JP-8 range molecules from Lignocellulosic Biomass). The views, opinions, and/or findings contained here are those of the authors and should not be interpreted as representing the official views or policies, either expressed or implied, of DARPA or the Department of Defense. In addition, this work was supported in part by the U.S. Department of Energy (DOE), Office of Basic Energy Sciences, and by the DOE Great Lakes Bioenergy Research Center (www.greatlakesbioenergy.org), which is supported by the U.S. DOE, Office of Science, Office of Biological and Environmental Research, through Cooperative Agreement between The Board of Regents of the University of Wisconsin System and the U.S. DOE. A patent application has been filed in association with the Wisconsin Alumni Research Foundation based on the technology reported here. We thank R. Oakes, T. Reigle, and C. Skadahl for their assistance in our investigation of the production of butene from GVL.

Supporting Online Material

www.sciencemag.org/cgi/content/full/327/5969/1110/DC1
Materials and Methods
Figs. S1 to S4
Tables S1 and S2

6 November 2009; accepted 7 January 2010
10.1126/science.1184362

Reconstructing Past Seawater Mg/Ca and Sr/Ca from Mid-Ocean Ridge Flank Calcium Carbonate Veins

Rosalind M. Coggon,[1] Damon A. H. Teagle,[2]* Christopher E. Smith-Duque,[2] Jeffrey C. Alt,[3] Matthew J. Cooper[2]

Proxies for past seawater chemistry, such as Mg/Ca and Sr/Ca ratios, provide a record of the dynamic exchanges of elements between the solid Earth, the atmosphere, and the hydrosphere and the evolving influence of life. We estimated past oceanic Mg/Ca and Sr/Ca ratios from suites of 1.6- to 170-million-year-old calcium carbonate veins that had precipitated from seawater-derived fluids in ocean ridge flank basalts. Our data indicate that before the Neogene, oceanic Mg/Ca and Sr/Ca ratios were lower than in the modern ocean. Decreased ocean spreading since the Cretaceous and the resulting slow reduction in ocean crustal hydrothermal exchange throughout the early Tertiary may explain the recent rise in these ratios.

Cation ratios in seawater reflect the balance between their supply to and removal from the oceans, and these ratios can control important geochemical processes. For example, the influence of the seawater Mg/Ca ratio on calcium carbonate ($CaCO_3$) precipitation [high Mg/Ca ratios favor the formation of aragonite, whereas low Mg/Ca ratios favor calcite (*1*)] has important effects on marine biota and the distribution of carbonate sediments. Seawater chemistry has varied with global climate throughout Earth's history, making past seawater cation ratios such as Mg/Ca and Sr/Ca attractive proxies for determining paleo-ocean conditions (*2*–*4*). Previous estimates of seawater cation ratios have been developed from mass-balance modeling (*5*, *6*) and analyses of marine cements (*7*), fossils (*8*–*10*), and fluid inclusions trapped in halite (*11*–*13*). Unfortunately, marine sedimentary carbonates are susceptible to diagenesis (*14*), and reactions during halite formation may perturb elemental ratios from those of contemporaneous seawater, requiring careful sample selection and analysis (*11*).

Here we propose a new method for reconstructing past variations in seawater Mg/Ca and Sr/Ca ratios from the composition of $CaCO_3$ veins (CCVs) formed in oceanic crust, as recovered by ocean drilling (*15*). CCVs are formed as seawater flows through the upper ocean crust on mid-ocean ridge flanks and reacts with basalt (*16*). Calcite and aragonite precipitate from these fluids to form veins within the basement lavas (*17*). The cation composition of the carbonates therefore records the chemistry of the basement fluid, provided that the temperature at which the veins formed can be determined and the temperature dependence of element partitioning between fluid and mineral is known (*15*, *18*).

If CCVs form on ridge flanks with thin sediment cover at near-bottom water temperatures (<6°C), the reaction between seawater and basalt is minimal and the carbonate data define the seawater Mg/Ca and Sr/Ca ratios at the age determined by their $^{87}Sr/^{86}Sr$ ratios and the well-established seawater Sr isotope record (*19*). However, if CCVs form at moderate tem-

[1]Department of Earth Science and Engineering, Imperial College London, South Kensington Campus, Exhibition Road, London SW7 2AZ, UK. [2]School of Ocean and Earth Science, National Oceanography Centre, University of Southampton, Southampton SO14 3ZH, UK. [3]Department of Geological Sciences, University of Michigan, Ann Arbor, MI 48109-1005, USA.

*To whom correspondence should be addressed. E-mail: damon.teagle@soton.ac.uk